

#### **PAPER • OPEN ACCESS**

# Light scattering by spatially dispersive semiconducting cylinders

To cite this article: Rhys Holmes et al 2025 J. Opt. 27 115601

View the article online for updates and enhancements.

## You may also like

- Shockingly Bright Warm Carbon Monoxide Molecular Features in the Supernova Remnant Cassiopeia A Revealed by JWST J. Rho, S.-H. Park, R. Arendt et al.
- ATLAAS: an automatic decision treebased learning algorithm for advanced image segmentation in positron emission

Beatrice Berthon, Christopher Marshall, Mererid Evans et al.

- Assessment of Damage Detection in Composite Structures Using 3D Vibrometry S Grigg, M Pearson, R Marks et al.

J. Opt. 27 (2025) 115601 (10pp)

# Light scattering by spatially dispersive semiconducting cylinders

Rhys Holmes<sup>1</sup>, Amal Aldhubaib<sup>1,2</sup>, Egor A Muljarov<sup>1</sup>, Wolfgang Langbein<sup>1</sup> and Hai-Yao Deng<sup>1,\*</sup>

- <sup>1</sup> School of Physics and Astronomy, Cardiff University, 5 The Parade, Cardiff CF24 3AA, Wales, United Kingdom
- <sup>2</sup> Department of Physics, Qassim University, Buraidah 51452, Al-Qassim, Saudi Arabia

E-mail: DengH4@cardiff.ac.uk

Received 11 June 2025, revised 17 September 2025 Accepted for publication 13 October 2025 Published 3 November 2025



#### **Abstract**

The scattering of light by cylindrical dielectrics is an old problem of wide interest. Most existing works assume spatially non-dispersive dielectrics characterized by a dielectric constant independent of wavenumber. Here we revisit the problem treating spatially dispersive semiconducting cylinders. We calculate the extinction, absorption and scattering cross sections as a function of the cylinder size and light frequency, depending on the properties of the cylinder boundary. Our calculations are based on a recently proposed theory without the use of additional boundary conditions. The results show that the cross sections strongly depend on how the cylinder surface scatters polarization waves, especially for small cylinders of radius much less than the light wavelength.

Keywords: Light scattering, spatially dispersive materials, additional boundary conditions

#### 1. Introduction

The study of the scattering of electromagnetic waves by infinitely long dielectric cylinders has accumulated an extensive literature [1], starting with Lord Rayleigh's work over a century ago [2]. It presents one of the few electromagnetic problems where rigorous analytical solutions could be obtained [3, 4]. More recently, the solutions were extended to treat sharp plasmonic resonances [5] and charged dielectric cylinders [6]. Beyond their fundamental importance, these rigorous solutions have also lent themselves to practical applications [7]. However, most existing works assume cylinders

Original Content from this work may be used under the terms of the Creative Commons Attribution 4.0 licence. Any further distribution of this work must maintain attribution to the author(s) and the title of the work, journal citation and DOI.

made of spatially non-dispersive dielectrics, which are characterized by a dielectric constant independent of wave vector, with few exceptions [8, 9].

Here we study light scattering by spatially dispersive cylinders, e.g. a semiconducting cylinder near excitonic resonances. As well known [10, 11], close to the excitonic resonance the dielectric properties of a semiconductor are described by spatially dispersive dielectric functions, which depend on both frequency and wave vector. Such spatial dispersion arises from the center-of-mass motions of the excitons. A conceptual hurdle, first encountered by Pekar in 1957 [12], relates to the polariton waves in the medium; As a result of spatial dispersion, these waves are admitted in more than one propagating modes with the same frequency and polarization. Consequently, the usual Maxwell's boundary conditions are insufficient for determining the amplitudes of the scattered waves. As a way out, Pekar supplemented Maxwell's boundary conditions with additional boundary conditions (ABCs), which have since been widely used [8, 9, 13]. However, the domain of validity of the ABC approach remains obscure [11, 14-16] and alternative approaches have been

<sup>\*</sup> Author to whom any correspondence should be addressed.

proposed [17–29]. Recently [30, 31], we showed that ABCs failed to capture the effects due to the propagation of polarization waves in thin films and ABC parameters devoid of physical meanings. Rather, a surface is physically characterized by a surface scattering amplitude (SSA), whose form depends on the microscopic material details and geometry. For planar surfaces the SSAs have been calculated for a model dielectric [31]. Here, the properties of SSAs for cylindrical surfaces are derived, and an explicit form is obtained for a simple surface model, which is then used to study light scattering by spatially dispersive cylinders. When implemented for cylinders, the ABC parameter comes with unrealistic curvature dependence.

The paper is organized as follows. In section 2, we describe the system and derive the SSA for cylindrical surfaces, and show that it is independent of cylinder curvature. In section 3, the scattering of light by cylinders is solved analytically and, in section 4, numerical illustrations are presented with material parameters suitable for the semiconductor GaAs at low temperatures. First the non-dispersive case is revisited to elucidate the method; then the dispersive case is solved. Analytical expressions for the cross sections are obtained in terms of the scattering amplitudes. Connections with ABCs are discussed in section 5 and the paper is concluded in section 6.

#### 2. SSA for cylindrical walls

The cylinder under consideration has a radius  $\rho$  and is extended infinitely along its axis coinciding with the z-axis; see figure 1. The dielectric response of the cylinder is described by its susceptibility,  $S(\mathbf{x}, \mathbf{x}')$ , by which the polarization in the cylinder is given by  $P(x) = \int d^3x' S(x,x') E(x')$ , where E(x)denotes the electric field that induces the polarization, while  $\mathbf{x} = (x, y, z)$  and  $\mathbf{x}' = (x', y', z')$  are points in the cylinder. Here and henceforth we assume that the electric field oscillates at frequency  $\omega$  by the factor  $e^{-i\omega t}$ , which we omit for notational simplicity. Here t denotes time. Accordingly, the polarization field (implicitly) bears the same oscillation factor and  $S(\mathbf{x}, \mathbf{x}')$ specifies the responses at frequency  $\omega$ . By virtue of the translational symmetry along the cylinder axis, we may assume without loss of generality a plane wave with wavenumber  $k_z$ along the z-axis for the fields, i.e.  $P(x) = P(r)e^{ik_zz}$  and E(x) = $\mathbf{E}(\mathbf{r})e^{ik_zz}$ . One then finds  $\mathbf{P}(\mathbf{r}) = \int d^2\mathbf{r}' \ S(\mathbf{r},\mathbf{r}') \ \mathbf{E}(\mathbf{r}')$ , where  $S(\mathbf{r},\mathbf{r}') = \int dz \ S(\mathbf{r},\mathbf{r}',z-z')e^{-ik_z(z-z')}$  with  $S(\mathbf{r},\mathbf{r}',z-z') = \int dz \ S(\mathbf{r},\mathbf{r}',z-z')e^{-ik_z(z-z')}$  $S(\mathbf{x}, \mathbf{x}')$  displaying the z dependence explicitly, and  $\mathbf{r} = (x, y)$ and  $\mathbf{r}' = (x', y')$  are the projections of  $\mathbf{x}$  and  $\mathbf{x}'$ , respectively. Dependence of  $S(\mathbf{r}, \mathbf{r}')$  on  $k_z$  is implicit.

Near the excitonic resonances of the semiconducting cylinder,  $S(\mathbf{r}, \mathbf{r}')$  can be split into a spatially non-dispersive background contribution  $S_b\delta^2(\mathbf{r}-\mathbf{r}')$ , where  $S_b$  is a constant background susceptibility and  $\delta^2(\mathbf{r}-\mathbf{r}')$  is the Dirac function in 2D, and the contribution  $\tilde{S}(\mathbf{r}, \mathbf{r}')$  due to excitons. Hence

$$\mathbf{P}(\mathbf{r}) = S_b \mathbf{E}(\mathbf{r}) + \tilde{\mathbf{P}}(\mathbf{r}), \quad \tilde{\mathbf{P}}(\mathbf{r}) = \int d^2 \mathbf{r}' \, \tilde{S}(\mathbf{r}, \mathbf{r}') \, \mathbf{E}(\mathbf{r}').$$

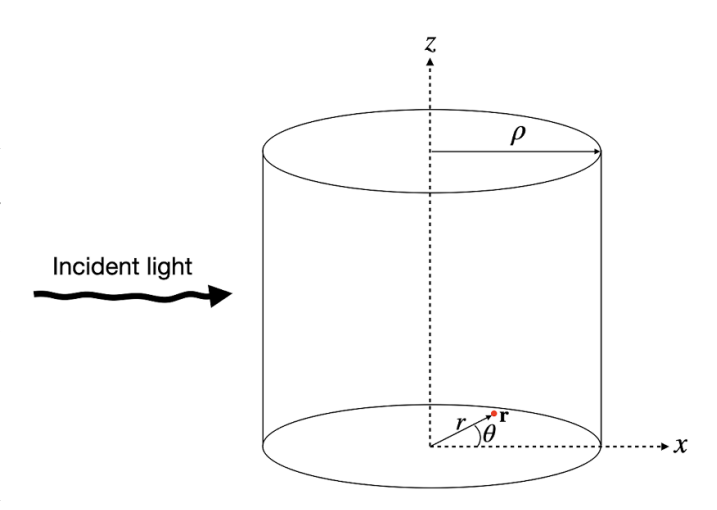


**Figure 1.** A dielectric cylinder of radius  $\rho$  extending along the z-axis is illuminated by a light wave.  $\mathbf{r} = (x, y) = r(\cos \theta, \sin \theta)$ .

According to the Lorentz oscillator model, which takes care of the ground exciton state but neglects higher-energy states [15, 30],  $\tilde{S}(\mathbf{r}, \mathbf{r}')$  satisfies the inhomogeneous Helmholtz equation,

$$\left(\partial_{\mathbf{r}}^{2}+q^{2}\right)\tilde{S}(\mathbf{r},\mathbf{r}')=-\frac{Q^{2}}{4\pi}\delta^{2}(\mathbf{r}-\mathbf{r}'),\quad q^{2}=\tilde{q}^{2}-k_{z}^{2},\quad(2)$$

where  $Q = \sqrt{2M\Delta/\hbar^2}$  and  $\tilde{q} = \sqrt{2M(\omega - \omega_{ex} + i\gamma)/\hbar}$  with  $\Delta, \omega_{ex}, M$  and  $\gamma$  being the exciton longitudinal-transverse splitting, transition energy, effective mass and damping rate, respectively, and  $\hbar$  is the reduced Planck constant.

Taking advantage of the rotational symmetry about the z-axis, we write  $x = r\cos\theta$  and  $y = r\sin\theta$ , where  $r = |\mathbf{r}|$  and  $\theta$  is the polar angle, and  $\tilde{S}(\mathbf{r}, \mathbf{r}')$  depends on  $\theta - \theta'$  rather than on  $\theta$  and  $\theta'$  separately. We expand

$$\tilde{S}(\mathbf{r}, \mathbf{r}') = \frac{iQ^2}{8} \sum_{m=-\infty}^{\infty} \tilde{S}_m(r, r') \frac{e^{im(\theta - \theta')}}{2\pi}, \quad (3)$$

where, as can be shown by direct substitution of this expression into equation (2),  $\tilde{S}_m(r,r')$  satisfies the inhomogeneous Bessel equation (apart from a constant factor), i.e.

$$\left(\partial_r^2 + \frac{1}{r}\partial_r + q^2 - \frac{m^2}{r^2}\right)\tilde{S}_m(r,r') = \frac{2i}{\pi r'}\delta(r-r'). \tag{4}$$

This equation can readily be solved. As in [30] and [31],  $\tilde{S}_m(r,r')$  in general contains two parts,

$$\tilde{S}_m(r,r') = S_m(r,r') + \mathcal{R}_m S_m(r,\rho) S_m(\rho,r') / S_m(\rho,\rho), \quad (5)$$

where  $\mathcal{R}_m$  is a parameter characteristic of the cylinder surface (see below),  $J_m(x)$  is the *m*th order Bessel function, and

$$S_m(r,r') = \begin{cases} J_m(qr')H_m^{(1)}(qr), & \text{for } r \geqslant r' \\ H_m^{(1)}(qr')J_m(qr), & \text{for } r' \geqslant r \end{cases}$$
(6)

where  $H_m^{(1)}(x)$  denotes the *m*th order Hankel function of the first kind and  $\text{Im}(q) \ge 0$ . Physically,  $S_m(r,r')$  represents an

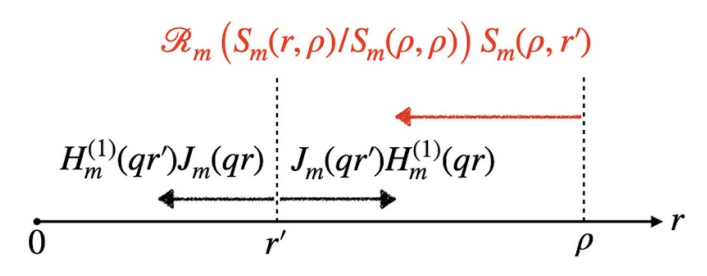


**Figure 2.** Illustration of  $\tilde{S}_m(r,r')$  as given by equation (5).

out-going polarization wave generated by a source electric field at r' while the second term in equation (5) represents the subsequent reflected polarization wave by the surface of the cylinder [30, 31]; See figure 2 for an illustration.  $S_m(r,r')$  is the same as for an infinite homogeneous system, i.e. the out-going free-space Green's function.

The parameter  $\mathcal{R}_m$  determines the relative amplitude for the reflected polarization wave and fully characterizes the property of the surface. In general, it is a function of  $\rho$  and r', i.e.  $\mathcal{R}_m = \mathcal{R}_m(\rho, r')$ , whose form depends on the surface details. The dependence on r' may be weak if the internal structure of the excitons can be ignored. Here we model the surface as a partially reflecting and partially absorbing sheath, by a parameter that characterizes the elastic scattering strength  $\lambda$ ; see appendix for details. For such a surface model,  $\mathcal{R}_m$  does not depend on r', which is then left out hereafter. We find

$$\mathcal{R}_{m}(\rho) = \frac{\bar{\lambda}S_{m}(\rho, \rho)}{1 - \bar{\lambda}S_{m}(\rho, \rho)}, \text{ with } \bar{\lambda} = \frac{i\pi}{2}\lambda\rho. \tag{7}$$

In the limit  $\lambda \to \infty$ , this gives  $\mathcal{R}_m = -1$  corresponding to the 'hard-wall' condition, by which  $\tilde{S}_m(\rho,r')=0$ . On the other hand, for  $\lambda=0$  the second term in equation (5) vanishes (i.e. the so-called 'dielectric approximation'), indicating a perfectly absorbing wall that thermalizes any incident polarization waves. As  $\mathcal{R}_m$  in equation (7) does not depend on r',  $\tilde{S}_m(r,r')$  becomes symmetric about r and r', i.e.  $\tilde{S}_m(r,r')=\tilde{S}_m(r',r)$ . However, we should note that this is not a universal feature.

In analogy to the case with a planar surface [30, 31], we define the large- $\rho$  limit of  $\mathcal{R}_m(\rho)$  as the SSA, denoted by  $\mathcal{R}$ , for the cylinder wall, i.e.  $\mathcal{R} = \lim_{\rho \to \infty} \mathcal{R}_m(\rho)$ . In this limit, the dependence on  $\rho$  and m due to the curvature of the wall should drop out (i.e.  $m/\rho$  vanishes). Using the large-argument approximation for Bessel and Hankel functions, one finds  $S_m(\rho,\rho) \approx (1/\pi \rho q) \left(1 + (-1)^{m+1} \mathrm{ie}^{2\mathrm{i}\rho q}\right)$ . For  $\mathrm{Im}(q)\rho \gg 1$ , this becomes  $S_m(\rho,\rho) \approx 1/\pi \rho q$  and hence

$$\mathcal{R}_m(
ho)pprox\mathcal{R}=rac{\mathrm{i}\lambda}{2q-\mathrm{i}\lambda}.$$

For GaAs [15],  $\text{Im}(q) \approx 10 \, \mu \text{m}^{-1}$  for  $\omega = \omega_{ex}$  and this approximation is valid if  $\rho$  is in excess of  $\sim 100 \, \text{nm}$ .

Also making use of the rotational symmetry, we expand the fields as

$$\mathbf{P}(\mathbf{r}) = \sum_{m=-\infty}^{\infty} \mathbf{P}_m(r) \frac{e^{im\theta}}{\sqrt{2\pi}}, \quad \mathbf{E}(\mathbf{r}) = \sum_{m=-\infty}^{\infty} \mathbf{E}_m(r) \frac{e^{im\theta}}{\sqrt{2\pi}},$$
(8)

where  $\mathbf{P}_m(r)$  and  $\mathbf{E}_m(r)$  are coefficients. Substituting these into equation (1) and making use of equations (3), (5) and (6) yield

$$\mathbf{P}_{m}(r) = S_{b}\mathbf{E}_{m}(r) + \tilde{\mathbf{P}}_{m}(r), \qquad (9)$$

where the excitonic contribution is given by

$$\tilde{\mathbf{P}}_{m}(r) = \frac{\mathrm{i}Q^{2}}{8} \int_{0}^{\rho} \mathrm{d}r' r' S_{m}(r, r') \mathbf{E}_{m}(r') 
+ \frac{\mathrm{i}Q^{2}}{8} \mathcal{R}_{m}(\rho) \frac{J_{m}(qr)}{J_{m}(q\rho)} \int_{0}^{\rho} \mathrm{d}r' r' S_{m}(\rho, r') \mathbf{E}_{m}(r').$$
(10)

equation (10) fully determines the spatially dispersive responses of the cylinder (including boundary effects).

#### 3. Light scattering by dielectric cylinders

For simplicity, we consider a light wave with wavenumber  $k_0 = \omega/c$ , where c is the speed of light in vacuum, normally incident upon the cylinder, i.e.  $k_z = 0$ . Oblique incidence with  $k_z \neq 0$  requires full treatment of the vector nature of the waves, and will be dealt with elsewhere. Further, we let the incident wave be linearly polarized along the z-axis. Consequently, both the electric field and the polarization field are directed along the z-axis,  $\mathbf{E}(\mathbf{r}) = (0,0,E(\mathbf{r}))$ ,  $\mathbf{P}(\mathbf{r}) = (0,0,P(\mathbf{r}))$  and  $\tilde{\mathbf{P}}(\mathbf{r}) = (0,0,\tilde{P}(\mathbf{r}))$ . One may write  $E(\mathbf{r})$  as a superposition of the incident field,  $E_{\rm in}(\mathbf{r}) = \mathrm{e}^{\mathrm{i}k_0x}$ , and the scattered field [30]; In Gaussian units,

$$E(\mathbf{r}) = E_{\rm in}(\mathbf{r}) - 4\pi k_0^2 \int d^2 \mathbf{r}' G(\mathbf{r} - \mathbf{r}') P(\mathbf{r}'), \qquad (11)$$

where the second term stands for the scattered field  $E_s(\mathbf{r})$  (waves emanated by the electric polarization in the cylinder) and  $G(\mathbf{r} - \mathbf{r}')$  is the Green's function of the Helmholtz equation satisfying out-going wave boundary condition,

$$\left(\partial_{\mathbf{r}}^{2} + k_{0}^{2}\right) G(\mathbf{r} - \mathbf{r}') = \delta^{2} \left(\mathbf{r} - \mathbf{r}'\right). \tag{12}$$

Again making use of rotational symmetry, we expand

$$G(\mathbf{r} - \mathbf{r}') = \sum_{m = -\infty}^{\infty} G_m(r, r') \frac{e^{\mathrm{i}m(\theta - \theta')}}{2\pi}$$
(13)

with the coefficient functions given by

$$G_m(r,r') = \frac{\pi}{2i} \begin{cases} J_m(k_0 r') H_m^{(1)}(k_0 r), & \text{for } r \geqslant r' \\ H_m^{(1)}(k_0 r') J_m(k_0 r), & \text{for } r' \geqslant r \end{cases},$$
(14)

which is the same as the expression for  $S_m(r,r')$  except for a constant prefactor. Substituting the expansion (8) into (11), we obtain

$$E_{m}(r) = E_{\text{in},m}(r) - 4\pi k_{0}^{2} \int_{0}^{\rho} dr' r' G_{m}(r,r') P_{m}(r'), \quad (15)$$

where  $E_{\text{in},m}(r) = d_m J_m(k_0 r)$  with  $d_m = i^m$  being the expansion coefficients of the plane incident wave, i.e.  $E_{\text{in}}(\mathbf{r}) = e^{\mathrm{i}k_0 r \cos \theta} =$ 

 $\sum_{m} E_{\text{in},m}(r) e^{im\theta}$ . Now equation (15) closes (9) and (10). They can be solved analytically, as shown below.

From an experimental point of view, it is particularly interesting how much incident energy is absorbed by the cylinder. For this purpose, we evaluate the Poynting vector  $\mathbf{S} = (c/2)\mathrm{Re}(\mathbf{E} \times \mathbf{B}^*)$ , where  $\mathbf{B} = -(\mathrm{i}/k_0)\nabla \times \mathbf{E}$  is the magnetic field. Considering that  $\mathbf{E} = (0,0,E)$ , we obtain  $\mathbf{B} = -(\mathrm{i}/k_0)(\partial_\nu E, -\partial_x E, 0)$  and

$$\mathbf{S}(r,\theta) = -\frac{c}{2k_0} \operatorname{Im}\left(E(\mathbf{r})\left(\partial_x E^*(\mathbf{r}), \partial_y E^*(\mathbf{r}), 0\right)\right). \tag{16}$$

The energy absorbed per unit time per unit length of the cylinder,  $W_a$ , is then given by the total energy flux through the surface of a virtual cylinder of unit length concentric with but having a larger radius than the actual cylinder [32], i.e.

$$W_a = -r_0 \int_0^{2\pi} d\theta \,\, \hat{\mathbf{r}} \cdot \mathbf{S}(r_0, \theta) \,, \tag{17}$$

where  $r_0 > \rho$  is the radius of the virtual cylinder and  $\hat{\mathbf{r}} = (\cos\theta, \sin\theta, 0)$  denotes the outward normal. One may let  $r_0$  be very large. For any stable system,  $W_a$  is positive and such system is an energy sink (i.e. energy is absorbed not emitted). The absorption cross section can now be written as  $\sigma_a = W_a/|\mathbf{S}_{\rm in}|$ , where  $\mathbf{S}_{\rm in}$  is the energy flux density carried by the incidence beam and is obtained from equation (16) with  $E_{\rm in}(\mathbf{r})$  in place of  $E(\mathbf{r})$ . We have chosen  $E_{\rm in}$  with unit amplitude so the energy density appears dimensionless and the cross sections  $\sigma_a$  and  $\sigma_s$  have the dimension of length rather than area, as  $W_a$  ( $W_s$ ) represent the energy absorbed (scattered) per unit time per unit length (not just per unit time).

One finds  $S_{in} = (c/2)(1,0,0)$ . It follows that

$$\sigma_a = \frac{r_0}{k_0} \operatorname{Im} \left[ \sum_{m = -\infty}^{\infty} E_m(r) \, \partial_r E_m^*(r) \right]_{r = r_0}. \tag{18}$$

In addition to  $\sigma_a$ , the scattering cross section  $\sigma_s$  is also of experimental interest.  $\sigma_s$  is the energy flux through the virtual cylindrical surface carried by the scattered waves, obtained from equation (18) with a sign change and  $E_m(r)$  replaced with  $E_{s,m}(r)$ , where  $E_{s,m}(r)$  is the scattered field amounting to the second term in equation (15),

$$\sigma_s = -\frac{r_0}{k_0} \operatorname{Im} \left[ \sum_{m=-\infty}^{\infty} E_{s,m}(r) \, \partial_r E_{s,m}^*(r) \right]_{r=r_s}. \tag{19}$$

Finally,  $\sigma_e = \sigma_a + \sigma_s$  is called the extinction cross section and describes the total loss of energy flux per unit length along the cylinder.

### 3.1. The non-dispersive case: $\tilde{P}(\mathbf{r})=0$

We proceed to solve the coupled equations (9) and (15). As an elucidation of the method, we first solve the non-dispersive case having no excitonic contribution,  $\tilde{P}(\mathbf{r}) = 0$ . Then  $P_m(r) = S_b E_m(r)$ , which using equation (15) yields

$$E_m(r) = E_{\text{in},m}(r) - 4\pi S_b k_0^2 \int_0^\rho dr' r' G_m(r,r') E_m(r'). \quad (20)$$

Outside the cylinder, using expression (14) for  $G_m(r,r')$ ,

$$E_{m}(r > \rho) = E_{\text{in},m}(r) + E_{s,m}(r)$$
, with  $E_{s,m}(r) = a_{m}H_{m}^{(1)}(k_{0}r)$ , (21)

where  $a_m$  is given by

$$a_{m} = 2\pi^{2} i S_{b} k_{0}^{2} \int_{0}^{\rho} dr' r' J_{m}(k_{0}r') E_{m}(r').$$
 (22)

To find the field inside the cylinder, we make the ansatz

$$E_m(r \leqslant \rho) = E_m J_m(kr), \qquad (23)$$

where  $E_m$  is an amplitude and k is some wavenumber. The ansatz is the cylindrical analog to the one we employed in [30] for a planar surface. Substituting the ansatz into equation (20) and after some algebra, one obtains [33]

$$k = \sqrt{\epsilon_b} k_0$$
, with  $\epsilon_b = 1 + 4\pi S_b$ , (24)

showing that the wavenumber k is given by the refractive index  $\sqrt{\epsilon_b}$ , where  $\epsilon_b$  is the dielectric constant, in agreement with the extinction theorem [17]. In addition, one finds

$$E_{m} = \frac{2d_{m}}{i\pi \rho} \frac{1}{\lambda_{m}^{(1)}(k, k_{0}; \rho)},$$
(25)

where we have introduced

$$\lambda_{m}^{(1)}(k,k_{0};\rho) = k_{0}H_{m+1}^{(1)}(k_{0}\rho)J_{m}(k\rho) - kH_{m}^{(1)}(k_{0}\rho)J_{m+1}(k\rho).$$
(26)

With this result and the ansatz, the integral in equation (22) can be performed [33] to obtain

$$a_{m} = \frac{\pi \rho}{2i} E_{m} \lambda_{m}^{(2)}(k, k_{0}; \rho) = i^{m-2} \frac{\lambda_{m}^{(2)}(k, k_{0}; \rho)}{\lambda_{m}^{(1)}(k, k_{0}; \rho)},$$
(27)

where we have introduced

$$\lambda_{m}^{(2)}(k,k_{0};\rho) = k_{0}J_{m+1}(k_{0}\rho)J_{m}(k\rho) - kJ_{m}(k_{0}\rho)J_{m+1}(k\rho).$$
(28)

Note that the poles of  $a_m$ , which occur at  $\lambda_m^{(1)}(k, k_0; \rho) = 0$ , determine the cylindrical modes of the system [3].

To summarize, we have found that

$$E_{m}(r) = d_{m} \times \begin{cases} \frac{2}{i\pi\rho} \frac{1}{\lambda_{m}^{(1)}(k,k_{0};\rho)} J_{m}(kr), & \text{for } r \leqslant \rho \\ J_{m}(k_{0}r) - \frac{\lambda_{m}^{(2)}(k,k_{0};\rho)}{\lambda_{m}^{(1)}(k,k_{0};\rho)} H_{m}^{(1)}(k_{0}r) & \text{for } r \geqslant \rho \end{cases}$$
(29)

We note that in the limit  $S_b \to 0$  and hence  $k \to k_0$ ,  $k_0^{-1}\lambda_m^{(1)}$  reduces to the Wronskian  $W[H_m^{(1)}(z),J_m(z)]$  between  $H_m^{(1)}(z)$  and  $J_m(z)$  evaluated at  $z=k_0\rho$ . Using the result [33]  $W[H_m^{(1)}(z),J_m(z)]=2/(\mathrm{i}\pi z)$ , we find  $\lambda_m^{(1)}(k_0,k_0;\rho)=\frac{2}{\mathrm{i}\pi\rho}$ . Meanwhile  $\lambda^{(2)}(k_0,k_0;\rho)=0$ . Thus,  $E_m(r)$  reduces to  $E_{\mathrm{in},m}(r)$  everywhere for  $S_b=0$ , signifying the absence of scattering.

#### 3.2. The dispersive case: $\tilde{P}(\mathbf{r}) \neq 0$

The equations to be solved are (9) and (15) supplemented by (10). We combine (9) and (10) for the *z*-component, yielding

$$P_{m}(r) = S_{b}E_{m}(r) + \frac{iQ^{2}}{8} \int_{0}^{\rho} dr' r' S_{m}(r, r') E_{m}(r') + \frac{iQ^{2}\mathcal{R}_{m}(\rho)}{8J_{m}(q\rho)} \cdot J_{m}(qr) \cdot \int_{0}^{\rho} dr' r' S_{m}(\rho, r') E_{m}(r').$$
(30)

This equation is to be solved together with equation (15). Consistent with the mirror symmetry about the x-z plane, one notes that  $E_{-m}(r) = (-1)^m E_m(r)$  and  $P_{-m}(r) = (-1)^m P_m(r)$ .

We proceed in the same way as we did for the nondispersive case. From equation (15), the electric field outside the cylinder can be written as

$$E_m(r \geqslant \rho) = E_{\text{in},m}(r) + E_{s,m}(r), \quad E_{s,m}(r) = b_m H_m^{(1)}(k_0 r),$$
(31)

where  $b_m$  is the coefficient for the scattered field, given by

$$b_{m} = 2\pi^{2} i k_{0}^{2} \int_{0}^{\rho} dr' r' J_{m}(k_{0}r') P_{m}(r').$$
 (32)

Note that  $b_{-m} = b_m$  due to rotational symmetry. To find the field inside the cylinder, we generalize the ansatz (23) to

$$E_{m}(r \leqslant \rho) = \sum_{\nu} E_{m,\nu} J_{m}(k_{\nu}r), P_{m}(r \leqslant \rho) = \sum_{\nu} P_{m,\nu} J_{m}(k_{\nu}r),$$
(33)

where the coefficients  $E_{m,\nu}$  and  $P_{m,\nu}$  are to be found selfconsistently together with the wavenumber  $k_{\nu}$  with  $\nu$  numbering the solutions. One may note that  $E_{-m,\nu} = E_{m,\nu}$  fulfilling rotational symmetry. Substituting the above ansatz into equation (30) and performing the integrals [33], we find

$$P_{m,\nu} = \left(S_b + \frac{1}{4\pi} \frac{Q^2}{k_\nu^2 - q^2}\right) E_{m,\nu},\tag{34}$$

where the quantity in the parenthesis represents the total polarizability for mode  $\nu$ , and

$$\sum_{n} \frac{Q^{2} E_{m,\nu}}{q^{2} - k_{\nu}^{2}} \left[ \bar{\mathcal{R}}_{m} \lambda_{m}^{(2)} \left( k_{\nu}, q; \rho \right) + \lambda_{m}^{(1)} \left( k_{\nu}, q; \rho \right) \right] = 0, \quad (35)$$

where  $\bar{\mathcal{R}}_m = \mathcal{R}_m(\rho) H_m^{(1)}(q\rho)/J_m(q\rho)$  contains the effects of spatial dispersion at the boundary. Substituting the ansatz (33) into equation (15) leads to

$$E_{m,\nu} = \frac{4\pi k_0^2}{k_{\nu}^2 - k_0^2} P_{m,\nu},\tag{36}$$

which, when combined with equation (34), determines the allowed values of  $k_{\nu}$  (see below), and

$$\sum \frac{4\pi k_0^2 \rho}{k_0^2 - k_{\nu}^2} \lambda_m^{(1)} (k_{\nu}, k_0; \rho) P_{m,\nu} = \frac{2id_m}{\pi}.$$
 (37)

Using equations (36) and (37) can be rewritten as

$$\sum_{\nu} \lambda_m^{(1)}(k_{\nu}, k_0; \rho) E_{m,\nu} = \frac{2d_m}{i\pi \rho}.$$
 (37')

In the above, the functions,  $\lambda_m^{(1)}(k_{\nu}, k_0; \rho)$  and  $\lambda_m^{(2)}(k_{\nu}, k_0; \rho)$ , are given by equations (26) and (28), respectively.

Equations (34)–(37') can readily be solved. Combining equations (34) and (36) produces

$$1 = \left(S_b + \frac{1}{4\pi} \frac{Q^2}{k_u^2 - q^2}\right) \frac{4\pi k_0^2}{k_u^2 - k_0^2}.$$
 (38)

This equation was also reached in [30], where planar boundaries were studied. Indeed, it is the same as for an infinite medium. The allowed values of  $k_{\nu}$  are then a property of the infinite medium regardless of the presence of boundaries, consistent with the extinction theorem [17], equation (38) is even in  $k_{\nu}$  so the solutions come in pairs, which we denote as  $k_1$ ,  $k_2$ , and  $k_3 = -k_1$ ,  $k_4 = -k_2$ . Their explicit expressions can be found in [30]. Note that  $J_m(-k_\nu r) = (-1)^m J_m(k_\nu r)$ . Hence  $J_m(k_1r)$  and  $J_m(k_3r)$  are not independent and neither are  $J_m(k_2r)$  and  $J_m(k_4r)$ . We therefore restrict ourselves to  $k_1$  and  $k_2$ , so that only four coefficients,  $E_{m,1}, E_{m,2}, P_{m,1}$  and  $P_{m,2}$ , need to be determined.  $P_{m,\nu}$  can be obtained from  $E_{m,\nu}$ via equation (34), while  $E_{m,1}$  and  $E_{m,2}$  are determined by equations (35) and (37'). We note that, in the absence of excitonic contribution (i.e. Q = 0), equation (35) is automatically fulfilled and equation (37') reproduces equation (25).

With the ansatz (33) and using equation (36), we can perform the integral in (32) to obtain the coefficient for the scattered field,

$$b_{m} = \frac{\pi \rho}{2i} \sum_{\nu} \lambda_{m}^{(2)}(k_{\nu}, k_{0}; \rho) E_{m,\nu}, \tag{39}$$

which is reminiscent of  $a_m$  [cf equation (27)] for the non-dispersive case. As is well known in wave scattering theory (see, e.g. [34]) and already mentioned, the poles of  $b_m$  (or  $a_m$  in the non-dispersive case) locate the electromagnetic modes (resonances) of the system.

The cross sections can be expressed in terms of  $d_m$  and  $b_m$ . To this end, we take the limit  $r_0 \to \infty$  in equations (18) and (19). Using identities involving derivatives of the Bessel and Hankel functions and their limiting forms at large arguments [33], one can readily show that

$$\begin{pmatrix} \sigma_s \\ \sigma_e \\ \sigma_a \end{pmatrix} = \frac{2}{\pi k_0} \sum_{m=-\infty}^{\infty} \begin{pmatrix} |b_m|^2 \\ -\operatorname{Re}(d_m b_m^*) \\ -\operatorname{Re}(d_m b_m^*) - |b_m|^2 \end{pmatrix}.$$
(40)

This result also applies to the non-dispersive case provided that  $b_m$  is replaced with  $a_m$  (see (27)), in which case one gets  $\sigma_a = 0$  if  $S_b$  (hence k) is real and there is no absorption.

#### 4. Numerical illustrations

Equations (35) and (37') can now be solved to obtain the coefficients  $E_{m,\nu}$ . We find

$$E_{m,\nu} = \frac{2d_m}{i\pi\rho} \frac{1}{\lambda_m^{(1)}(k_{\nu}, k_0; \rho) + \eta_m^{2\nu - 3} \lambda_m^{(1)}(k_{\bar{\nu}}, k_0; \rho)}, \quad (41)$$

where  $\bar{1} = 2$ ,  $\bar{2} = 1$ , and the quantity

$$\eta_{m} = \frac{k_{1}^{2} - q^{2}}{q^{2} - k_{2}^{2}} \cdot \frac{\bar{\mathcal{R}}_{m} \lambda_{m}^{(2)}(k_{2}, q; \rho) + \lambda_{m}^{(1)}(k_{2}, q; \rho)}{\bar{\mathcal{R}}_{m} \lambda_{m}^{(2)}(k_{1}, q; \rho) + \lambda_{m}^{(1)}(k_{1}, q; \rho)}$$
(42)

gives the ratio of  $E_{m,1}$  to  $E_{m,2}$ . These expressions can then be substituted in (39) to obtain the scattering amplitudes

$$b_{m} = i^{m-2} \cdot \sum_{\nu} \frac{\lambda_{m}^{(2)}(k_{\nu}, k_{0}; \rho)}{\lambda_{m}^{(1)}(k_{\nu}, k_{0}; \rho) + \eta_{m}^{2\nu-3} \lambda_{m}^{(1)}(k_{\bar{\nu}}, k_{0}; \rho)}, \quad (43)$$

from which the cross sections can be obtained via (40).

In numerical demonstrations, the summation over m in equation (40) needs a cut-off, i.e.  $|m| \leq m_c$ . Numerical convergence is achieved as soon as  $m_c$  exceeds  $\rho Q$ ; See [35] for a rigorous proof. Note that 1/Q represents the smallest length scale in the system.

In all of the numerical illustrations presented here, values for the physical parameters are adopted from reference [15], quoted here:  $\epsilon_b = 12.66$ ,  $\Delta = 0.086$  meV,  $M = 4.7 \times 10^{-31}$  Kg,  $\hbar \omega_{ex} = 1514.8$  meV and  $\hbar \gamma = 0.05$  meV, yielding  $Q^{-1} \approx 8.24$  nm. These values were representative of excitons in bulk GaAs. We normalize lengths (wave numbers) by 1/Q (Q) and frequency by  $\omega_{ex}$  for convenience. The cross sections per unit length,  $\sigma_a$ ,  $\sigma_s$  and  $\sigma_e$ , are therefore normalized by 1/Q as well. We then plot the dimensionless quantities,  $Q\sigma_a$ ,  $Q\sigma_s$  and  $Q\sigma_e$  instead.

In figure 3 we show  $|\eta_0|$  alongside the wavenumber for frequency near the exciton resonance  $\omega_{ex}$ , as measured by the detuning  $\delta = (\omega - \omega_{ex})/\Delta$ . It is seen that q approaches  $k_1$  for increasing  $\delta$  and consequently, from equation (42),  $|\eta_0| \propto |\frac{q^2-k_1^2}{q^2-k_2^2}|$  approaches zero leading to negligible  $E_{m,1}$ . On the other hand, with decreasing  $\delta$ , q approaches  $k_2$  and  $|\eta_m|$  approaches infinity, leading to negligible  $E_{m,2}$ . This implies that, at frequencies far away from  $\omega_{ex}$ , one may keep only the dominant mode and thus approximately restore the non-dispersive case, whereby  $b_m$  reduces to  $a_m$ . However, in the immediate proximity of  $\omega_{ex}$  (i.e.  $|\delta| \ll 1$ ), both modes are important and the system is highly dispersive. Similar features are also seen in  $\eta_{m\neq 0}$ .

For small cylinders with  $\rho$  less than or comparable to 1/Q, only the m=0 component contributes significantly. Then  $\sigma_s \approx \frac{2}{\pi k_0} |b_0|^2$  and  $\sigma_e \approx -\frac{2}{\pi k_0} \mathrm{Re}(b_0)$ . In figure 4 we show the cross sections for a cylinder with  $\rho Q=1$  at various values of the scattering strength  $\lambda$ . One may see that  $\sigma_a$  displays a step-like rise as  $\omega$  increases beyond the exciton resonance frequency  $\omega_{ex}$ . Also clear is that increasing  $\lambda$  strongly suppresses  $\sigma_a$ . These features seem more pronounced with smaller  $\rho$ . For example, in figure 5 we show  $\sigma_a$  for  $\rho Q=0.2$ , where the step-like rise and the suppression due to large  $\lambda$  in  $\sigma_a$  are very

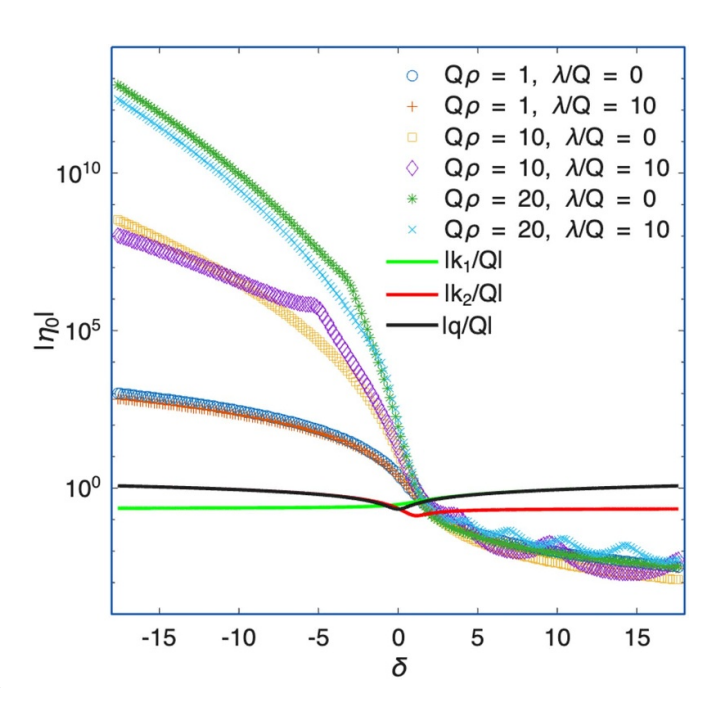


**Figure 3.**  $\eta_m$ , the ratio of  $E_{m,1}$  to  $E_{m,2}$ , against detuning  $\delta = (\omega - \omega_{ex})/\Delta$  at m = 0 for various values of  $\rho$  and  $\lambda$ . Also shown are  $k_1$ ,  $k_2$  and q.

clear. The suppression occurs because increasing  $\lambda$  decreases the polarization at the wall and consequently, the polarization everywhere in the cylinder must be decreased as the polarization varies little across the small radius. For small cylinders, there is little scattering so absorption makes the chief contribution to the extinction. Indeed, a small- $\rho$  analysis of  $b_0$  shows that  $\sigma_s \sim \rho^4$  while  $\sigma_a \sim \rho^2$ . As shown in the middle panel of figure 4,  $\sigma_s$  features a rounded singularity (a cusp) at  $\omega = \omega_{ex}$ , where  $q^2$  would be zero if not for dissipation (via  $\gamma$ ). This stems from the singular behaviors of  $H_0^{(1)}(q\rho)$  (contained in  $\bar{\mathcal{R}}_0$  [cf equation (42)]) at small arguments, i.e.  $H_0^{(1)}(q\rho) \sim (2\mathrm{i}/\pi) \ln(q\rho/2)$  for small  $q\rho$ .

For cylinders with  $\rho$  greater than 1/Q yet still sufficiently small so that the m = 0 component remains the most important contribution, the step-like feature is superseded by a gradual rise followed by some oscillations. Increasing  $\lambda$  enhances the oscillations but with diminishing impact as  $\rho$  increases. These features are seen in figure 6, where we show the results for  $\rho Q = 10$ . Note that this value of  $\rho$  is only a tiny fraction of the wavelength in vacuum,  $2\pi/k_0 \approx 100/Q$  of the incident light. Here we see that  $\sigma_s$  far exceeds  $\sigma_a$  and makes the chief contribution to  $\sigma_e$ . Peaks show up in  $\sigma_a$  on the shoulder with  $\omega > \omega_{ex}$  of the frequency window. To each peak, there corresponds a cusp in  $\sigma_s$ . These peaks are reminiscent of what occurs to planar structures such as slabs [30, 31] and they signify the repeated bounces of ring-shaped polarization wave packets by the cylinder wall. The spacing between successive peaks roughly equals  $2\pi$  divided by the time it takes for a wave packet to travel radially the distance of  $\rho$ , i.e.  $2\pi/(\rho/v_g) = 2\pi v_g/\rho$ , where  $v_g = d\omega/dq =$  $\sqrt{2\hbar(\omega-\omega_{ex})/M}$  gives the group velocity of the wave packet. Mathematically, this is understood as due to the oscillatory

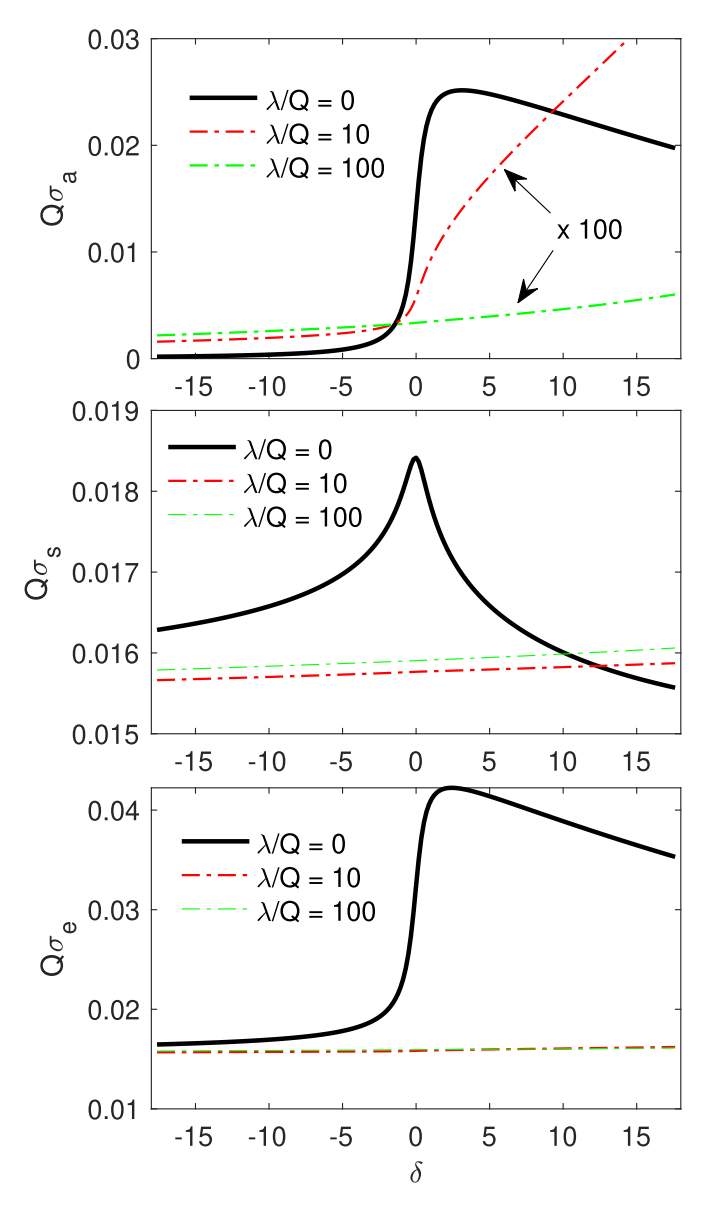


**Figure 4.** Cross sections,  $\sigma_a$ ,  $\sigma_s$  and  $\sigma_e$  versus  $\delta$  for  $\rho = 1/Q$  and various scattering strength  $\lambda$ .

nature of the cylindrical functions,  $H_0^{(1)}(q\rho)$  and  $J_0(q\rho)$  in the argument  $\rho q$ . The oscillation period is approximately  $2\pi$  for individual functions but less (about halved) for their product. For  $\omega < \omega_{ex}$  no such peaks exist since the polarization waves cannot propagate at these frequencies. i.e. q is mostly imaginary with only a negligible real part.

For large cylinders with  $\rho$  in great excess of 1/Q, the cross sections display another type of peaks on top of those due to bounces of polarization waves (which get increasingly obscure with increasing  $\rho$ ). These new peaks represent resonances that originate from the  $m \neq 0$  components of the polarization waves, which can be important as long as m is much less than  $\rho|q|$ . They appear for both  $\omega > \omega_{ex}$  and  $\omega < \omega_{ex}$ . Some examples are shown in figure 7. While surface scattering (via  $\lambda$ ) plays a less important role for larger cylinders, its influence is still visible near  $\omega_{ex}$ .

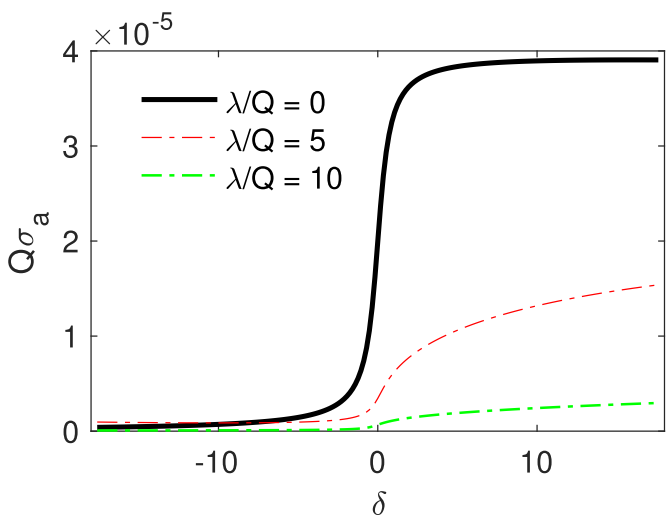


**Figure 5.** Step-like rise and suppression of the absorption cross section  $\sigma_a$  by increasing scattering strength  $\lambda$  for small cylinders.  $\rho = 0.2/Q$ .

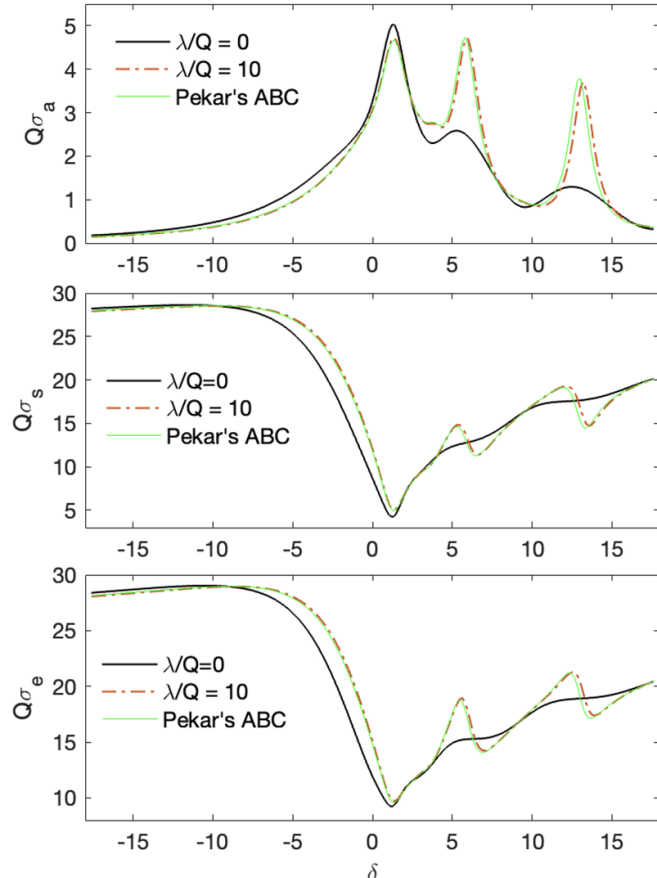


**Figure 6.** Same as figure 4 except that  $\rho = 10/Q$ . Oscillations on the shoulder  $\omega > \omega_{ex}$  signify polarization waves bounced back and forth at the wall (echo effect).

#### 5. Discussions

We here briefly discuss the ABC approach. In that approach, one might assume (i) that inside the cylinder  $E_m(r)$  and  $P_m(r)$ 

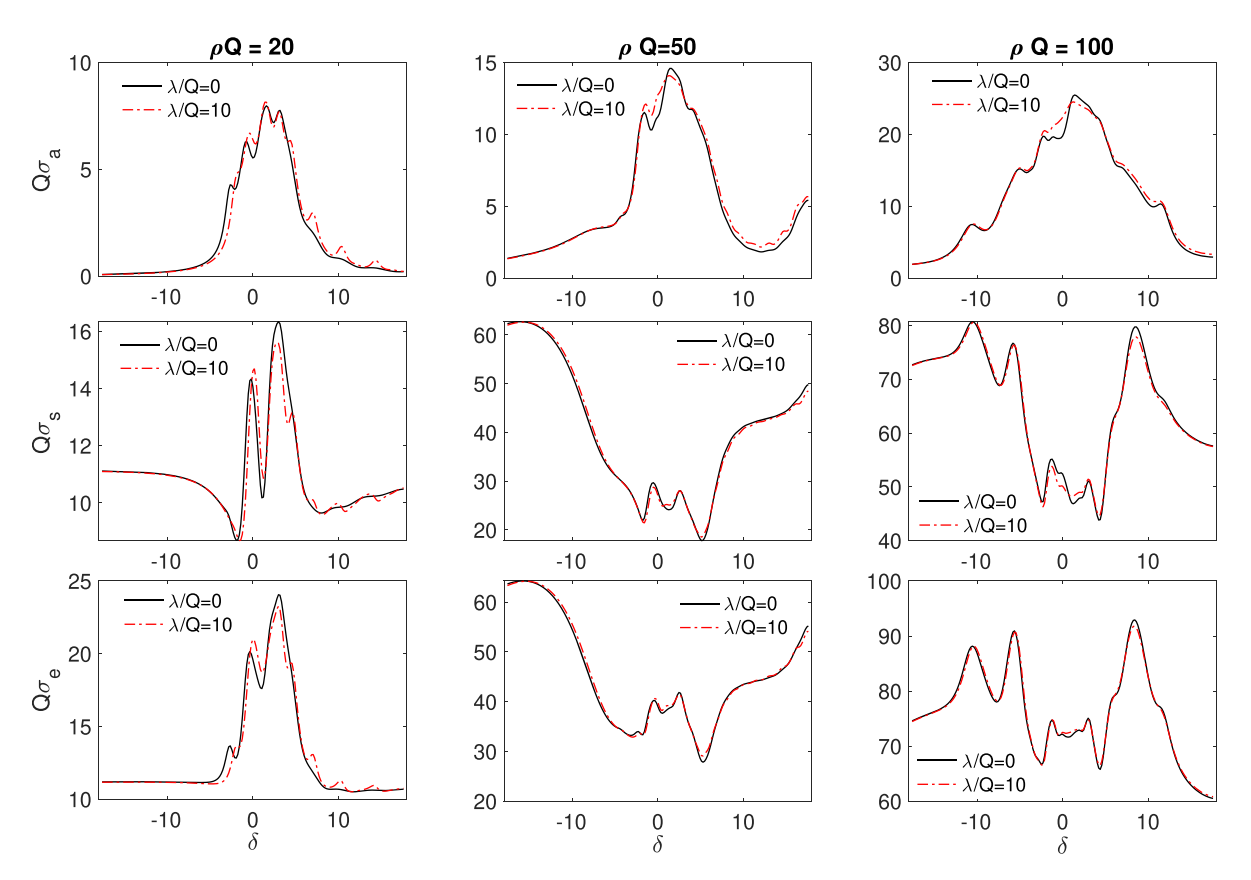


Figure 7. Cross sections,  $\sigma_a$ ,  $\sigma_s$  and  $\sigma_e$  versus  $\delta$  at various cylinder radius  $\rho = 20/Q$ , 50/Q, 100/Q and scattering strength  $\lambda$ . For large cylinders, the components with  $m \neq 0$  become pronounced leading to additional oscillations for both  $\omega > \omega_{ex}$  and  $\omega < \omega_{ex}$ .

take on the form prescribed in equation (33), and (ii) that the coefficients  $P_{m,\nu}$  and  $E_{m,nu}$  are related in the same way as in an infinite medium (i.e. equation (34)), and (iii) that the wave numbers  $k_{\nu}$  are the same as for an infinite medium (i.e. determined by equation (38)). In this way, one would end up with three unknowns for each angular number m:  $E_{m,1}, E_{m,2}$  and  $b_m$ . Note that the scattering amplitude  $b_m$  is the counterpart of the reflection coefficient in the case of semi-infinite medium. There are two Maxwell's boundary conditions: the continuity of  $E_m(r)$  and the continuity of the derivative of  $E_m(r)$  (or equivalently the continuity of the tangential component of the magnetic field), which are therefore inadequate to uniquely determine the three unknowns. As a remedy, one would then impose an ABC in the form that

$$\partial_r \tilde{P}_m(r) = \kappa_m \tilde{P}_m(r) \tag{44}$$

for  $r = \rho$ , where  $\tilde{P}_m(r)$  denotes the excitonic contribution to  $P_m(r)$  and  $\kappa_m$  is a parameter. Our theory allows us to calculate both  $\tilde{P}_m(r)$  and  $\partial_r \tilde{P}_m(r)$  and hence to determine  $\kappa_m$ . Straightforward manipulations give

$$\kappa_{m} = \frac{2i}{\pi \rho} \frac{1}{[1 + \mathcal{R}_{m}(\rho)] H_{m}^{(1)}(q\rho)} + q J_{m}'(q\rho), \qquad (45)$$

where  $J'_m(z) = \partial_z J_m(z)$ . This expression shows that  $\kappa_m$  depends on  $\rho$  and m even in the limit of very large  $\rho$ .

Actually, for  $\rho \to \infty$ ,  $H_m^{(1)}(q\rho) \sim \mathrm{e}^{\mathrm{i}q\rho}/\sqrt{\rho}$  and  $J_m'(q\rho) \sim \sin(q\rho - \pi/4 - m\pi/2)/\sqrt{\rho}$ , and thus  $\kappa_m \sim 1/\sqrt{\rho}$ . In contrast, at least for the specific model in equation (7),  $\mathcal{R}_m(\rho)$  becomes independent of both  $\rho$  and m in this limit. In view of this,  $\kappa_m$  is not a useful parameter for experimental studies and should not be interpreted as a surface property.

In [8] and [9], optical properties of spatially dispersive cylinders were studied using Pekar's ABC, i.e.  $\tilde{P}_m(\rho)=0$ , which corresponds to  $\lambda\to\infty$  (see figure 6 for a comparison). Results similar to figure 6 with oscillations for  $\delta>0$  were obtained, but their exciton model was not exactly the same as that used in the present work and hence further comparison is not pursued here.

Finally, one should not confound the SSA introduced here with the so-called d parameters introduced by Feibelman [36], which are also referred to as surface response functions sometimes. They have totally different physical meanings and are irrelevant in the macroscopic limit; see the Supplemental Material of [30] for further discussions.

#### 6. Conclusions

We have reported a theory for the optical response of spatially dispersive dielectric cylinders, exemplified for semiconductors at frequencies near an excitonic resonance. Consistent with the general theory presented in our previous work, we show

that the effects due to the cylinder wall are described by the SSA  $\mathcal{R}$ . We find that for small cylinders the scattering, absorption and extinction cross sections are highly sensitive to the value of  $\mathcal{R}$  (or equivalently the surface scattering strength  $\lambda$ ). Our numerical results may be of experimental interest as they are based on real material parameters, that of GaAs. The theory may find practical application in nano-photonic devices based on spatial and temporal dispersion effects [37, 38].

#### Data availability statement

The data cannot be made publicly available upon publication because no suitable repository exists for hosting data in this field of study. The data that support the findings of this study are available upon reasonable request from the authors.

#### Appendix. model for equation (7)

Here we present a model for equation (7). We start with equation (4). This equation is valid for r lying in the interior of the cylinder [30, 31], where boundary scattering does not exist. For simplicity, we account for such scattering by adding  $\lambda \delta(r-\rho)$  to the equation, where  $\lambda$  is a (generally complex) constant parameter, and obtain

$$\left(\partial_r^2 + \frac{1}{r}\partial_r + q^2 - \frac{m^2}{r^2} + \lambda\delta(r - \rho)\right)\tilde{S}_m(r, r') = \frac{2i}{\pi r'}\delta(r - r'),$$
(A.1)

which is valid also for r lying on the cylinder surface. It is noted that the thus-represented scattering is elastic with scattering strength  $\lambda$ . We can bring equation (A.1) into an integral form,

$$\int dr'' \left[ \mathcal{L}_0(r,r'') + V(r,r'') \right] \tilde{S}_m(r'',r') = \frac{2i}{\pi r'} \delta(r-r'),$$
(A.2)

where  $\mathcal{L}_0$  represents the kernel of the operator  $\partial_r^2 + \frac{1}{r}\partial_r + q^2 - \frac{m^2}{r^2}$  under usual out-going boundary conditions, satisfying

$$\int dr'' \mathcal{L}_0(r,r'') S_m(r'',r') = \frac{2i}{\pi r'} \delta(r-r'), \qquad (A.3)$$

and  $V(r,r') = \lambda \delta(r-\rho)\delta(r'-\rho)$ . According to general wave scattering theory [31], the solution to (A.2) can be written as

$$\tilde{S}_{m}(r,r') = S_{m}(r,r') + \int dr_{1} \int dr_{2} S_{m}(r,r_{1}) T(r_{1},r_{2}) S_{m}(r_{2},r'),$$
(A.4)

where T(r, r') denotes the scattering matrix given by

$$\begin{split} T\left(r,r'\right) &= \frac{\mathrm{i}\pi\,\rho}{2} V\!\left(r,r'\right) \\ &+ \left(\frac{\mathrm{i}\pi\,\rho}{2}\right)^2 \int \mathrm{d}r_1 \int \mathrm{d}r_2 V\!\left(r,r_1\right) S_m\left(r_1,r_2\right) V\!\left(r_2,r'\right) \\ &+ \left(\frac{\mathrm{i}\pi\,\rho}{2}\right)^3 \int \mathrm{d}r_1 \int \mathrm{d}r_2 \int \mathrm{d}r_3 \int \mathrm{d}r_4 \end{split}$$

$$\times V(r,r_1) S_m(r_1,r_2) V(r_2,r_3) S_m(r_3,r_4) V(r_4,r') + ...,$$
(A.5)

where the ellipsis stand for the higher-order terms in the series. Evaluating this expression leads to

$$T(r,r') = \frac{i\pi \lambda \rho/2}{1 - i(\pi \lambda \rho/2) S_m(\rho,\rho)} \delta(r-\rho) \delta(r'-\rho). \quad (A.6)$$

Using this expression in (A.4) and comparing the result to equation (5), one finds equation (7).

The above elastic scattering model, however, would allow polarization waves to leak out of the cylinder for any finite  $\lambda$ , which is unphysical. This issue may be avoided if the cylinder surface is allowed to absorb (i.e. dissipate) polarization waves, and  $\lambda$  is then treated as a parameter that measures how strongly polarization waves are elastically scattered. For finite  $\lambda$ , polarization waves are then partially scattered and partially absorbed. Such absorption could happen due to inelastic scattering with, for example, lattice vibrations, which can take energy from the polarization waves and thermalize them. A detailed microscopic treatment of inelastic scattering is beyond the scope of this work. In general,  $\lambda$ might depend on frequency but not on m nor  $\rho$  due to cylindrical symmetry. The dependence on frequency may be ignored as the frequency regime of interest is very narrow about the exciton resonance. All said, the as-described model remains a gross simplification of reality. A realistic functional form for  $\mathcal{R}_m(\rho, r')$  must account for the internal structure of excitons and may be developed along the lines sketched in the Supplemental Information of [30]. These issues are being studied.

#### **ORCID iDs**

#### References

- [1] van de Hulst H C 2003 *Light Scattering by Small Particles*Illustrated edn (Dover Publications Inc.)
- [2] Rayleigh L 1881 *Phil. Mag.* 12 81Rayleigh L 1918 *Phil. Mag.* 36 365
- [3] Stratton J A 2006 Electromagnetic Theory (Ieee Press Series) ed D G Dudley (Wiley)
- [4] Doost M B, Langbein W and Muljarov E A 2013 Phys. Rev. A 87 043827
- [5] Luk'yanchuk B S and Ternovsky V 2006 Phys. Rev. B 73 235432
- [6] Zhang S, Zhang W and Liu L 2020 J. Quant. Spectrosc. Radiat. Transfer 253 107167
- [7] Kienle A and Hibst R 2006 *Phys. Rev. Lett.* **97** 018104
- [8] Ruppin R 1989 J. Opt. Soc. Am. B 6 1559
- [9] Dub P 1991 Opt. Commun. 82 218
- [10] Hopfield J J 1958 Phys. Rev. 112 1555
- [11] Agranovich V M and Ginzburg V L 1966 Spatial Dispersion in Crystal Optics and the Theory of Excitons (Interscience)
- [12] Pekar S I 1957 Sov. Phys-JETP 6 785

- [13] See, for example Churchill R J and Philbin T G 2017 *Phys. Rev. B* **95** 205406 and references therein
- [14] Tignon J, Hasche T, Chemla D S, Schneider H C, Jahnke F and Koch S W 2000 Phys. Rev. Lett. 84 3382
- [15] Muljarov E A and Zimmermann R 2002 Phys. Rev. B 66 235319
- [16] Victor K, Axt V M and Stahl A 1993 Z. Phys. B 92 35
- [17] Pattanayak D N and Wolf E 1972 Opt. Commun. 6 217–20 Agarwal G S, Pattanayak D N and Wolf E 1971 Phys. Rev. Lett. 27 1022
- [18] Birman J L and Sein J J 1972 Phys. Rev. B 6 2482
- [19] Zeyher R, Birman J L and Brenig W 1972 Phys. Rev. B 6 4613
  Zeyher R, Birman J L and Brenig W 1972 Phys. Rev. B 6 4617
- [20] Agranovich V M and Yudson V I 1973 Opt. Commun. 7 121
- [21] Rimbey P R 1977 Phys. Rev. B 15 1215
- [22] Ruppin R and Englman R 1984 Phys. Rev. Lett. 53 1688Ruppin R 1986 J. Phys. France 47 259
- [23] Chen B and Nelson D F 1993 Phys. Rev. B 48 15365
- [24] Henneberger K 1998 Phys. Rev. Lett. **80** 2889
- [25] Nelson D F and Chen B 1999 Phys. Rev. Lett. 83 1263
- [26] Zeyher R 1999 Phys. Rev. Lett. 83 1264
- [27] Schmidt R and Scheel S 2016 Phys. Rev. A 93 033804

- [28] Deng H-Y 2020 Ann. Phys., NY 418 168204
   Deng H-Y 2020 Eur. J. Phys. 41 35203
   Praill S, Lawton C, Balable H and Deng H Y 2023 Solids 4 268
- [29] Brown D and Deng H-Y 2021 J. Chem. Phys. 155 114109
- [30] Deng H-Y and Muljarov E A 2022 Phys. Rev. B 106 195301
- [31] Wink S M, Muljarov E A, Langbein W and Deng H-Y 2023 Phys. Rev. B 108 245302
- [32] Jackson J D 1999 Classical Electrodynamics 3rd edn (Wiley)
- [33] F W J Olver, A B O Daalhuis, D W Lozier, B I Schneider, R F Boisvert, C W Clark, B R Miller, B V Saunders, H S Cohl and M A McClain (eds) 2025 Nist Digital Library of Mathematical Functions (online version) ch 10.22
- [34] Landau L D and Lifshitz E M 1999 *Quantum Mechanics*(Non-relativistic Theory) 3rd edn (Butterworth-Heinemann) ch 128
- [35] Abushagur M A G 1984 Scattering of Light From Large Cylinders (California Institute of Technology)
- [36] Feibelman P J 1982 Prog. Surf. Sci. 12 287
- [37] Fan Y, Huang W, Zhu F, Liu X, Jin C, Guo C, An Y, Kivshar Y, Qiu C-W and Li W 2024 *Nature* 630 77
- [38] Yang R et al 2023 Laser Photon. Rev. 17 2200975